

Mechanical response of 2024-7075 aluminium alloys joined by Friction Stir Welding

P. CAVALIERE*, E. CERRI

Department of "Ingegneria dell'Innovazione," Engineering Faculty, University of Lecce, Italy
E-mail: pasquale.cavaliere@unile.it

A. SQUILLACE

Department of Materials and Production Engineering, Engineering Faculty, University of Naples Federico II, Italy

The mechanical and microstructural properties of 2024 and 7075 aluminium alloys joined together by friction stir welding were analysed in the present study. The two materials were welded with perpendicular rolling direction and after were tested in tension at room temperature in order to analyse the mechanical response and to observe the differences with the parent materials, the tensile response of the material in longitudinal direction revealed an increase in strength respect to the transverse one. The cyclic fatigue tests were conducted in the axial direction with $R = \sigma_{\min}/\sigma_{\max} = 0.1$). The microstructure resulting from the FSW process was studied by employing optical and scanning electron microscopy.
© 2005 Springer Science + Business Media, Inc.

1. Introduction

Friction Stir Welding (FSW) is being targeted by the industry for structurally demanding applications to provide high-performance benefits. FSW is shown not to cause severe distortion and residual stresses generated are low compared to the traditional welding processes [1–3].

From a microstructural point of view the weld's very fine and equiaxed grain structure produces a higher mechanical strength and ductility [4–6]. Jata and Semiatin [7] showed that the microstructure in the weld nugget zone evolves through a continuous dynamical recrystallization process.

This new technology can join difficult to weld aluminium alloys by traditional fusion techniques, for example alloys belonging to the 2XXX series with limited weldability and the 7XXX series generally not recommended for welding, even if they are the more used aluminium alloys in aerospace applications [8–11]. Conventional welding, results in a dendritic structure in the fusion zone which lead to a drastic decrease of the

mechanical properties [11]. The FSW process is a solid state process and therefore solidification structure is absent in the weld and the problem related to the presence of brittle intrer-dendritic and eutectic phases is eliminated [12].

In addition, in FSW the surface oxide is not deterrent for the process; no particular cleaning operations are needed prior to welding.

Actually, Friction Stir Welding is mainly used for joining similar materials, even if few systematic studies have been performed to observe the effect of combination of alloys with different composition [13–15]. This is a core demand of Aircraft Industries to substitute the traditional joining technologies with low costs and high efficiency ones such as Friction Stir Welding in the future advanced design.

Another important aspect is the possibility to joint materials with very different mechanical and physical properties such as Aluminium-Steel [16], Aluminium-Magnesium [17], Aluminium-Silver [18].

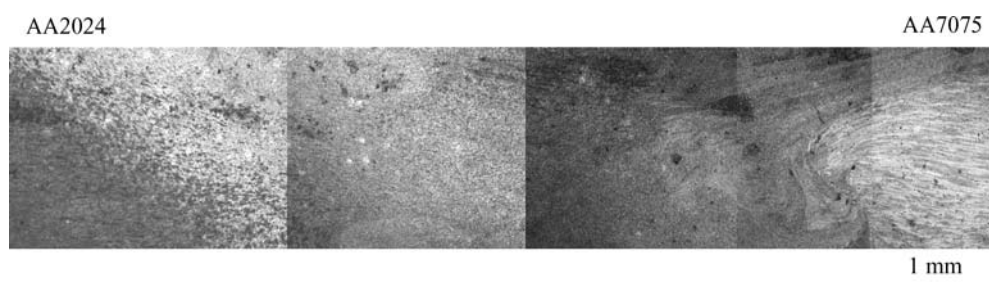


Figure 1 Optical micrograph of the cross-section of the studied joints.

*Author to whom all correspondence should be addressed.

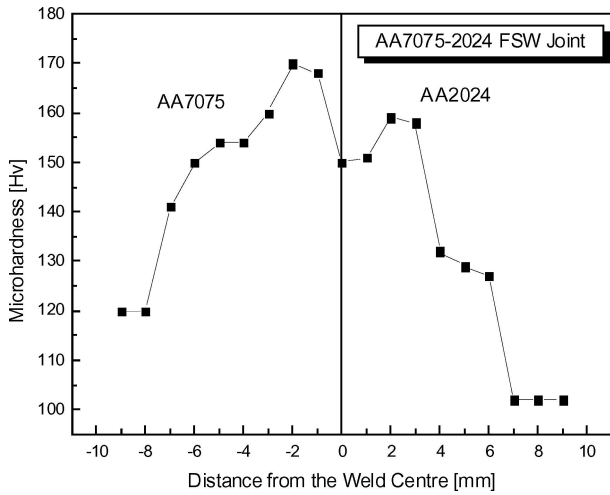


Figure 2 Microhardness profile measured in the joints of the 2024-7075 FSW plates, AA7075 on the left.

IN FSW the work piece does not reach the melting point and the mechanical properties of the welded zone are much higher compared to the traditional techniques, in fact, the undesirable microstructure resulting from melting and re-solidification, characterized by low mechanical properties, is absent in FS welds leading to improved mechanical properties such as ductility and strength in some alloys [19].

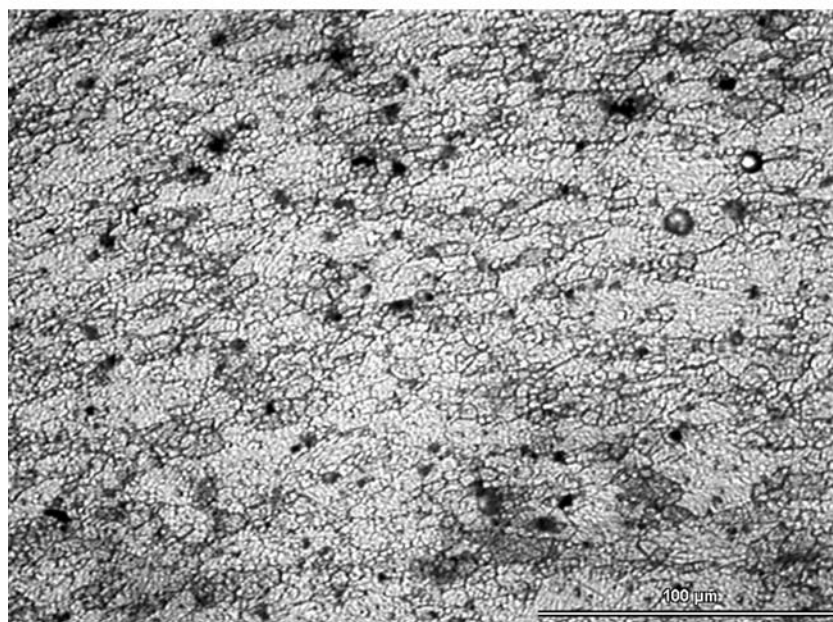
The aim of the present study is to show the mechanical properties of FSW of 2024 aluminium alloy in T3 condition and 7075 in T6 condition with perpendicular rolling direction.

2. Experimental procedure

The welds for the present study were prepared by Friction Stir Welding a sheet of 2024 Al alloy in the T3 condition and a sheet of 7075 Al alloy in the T6



(a)



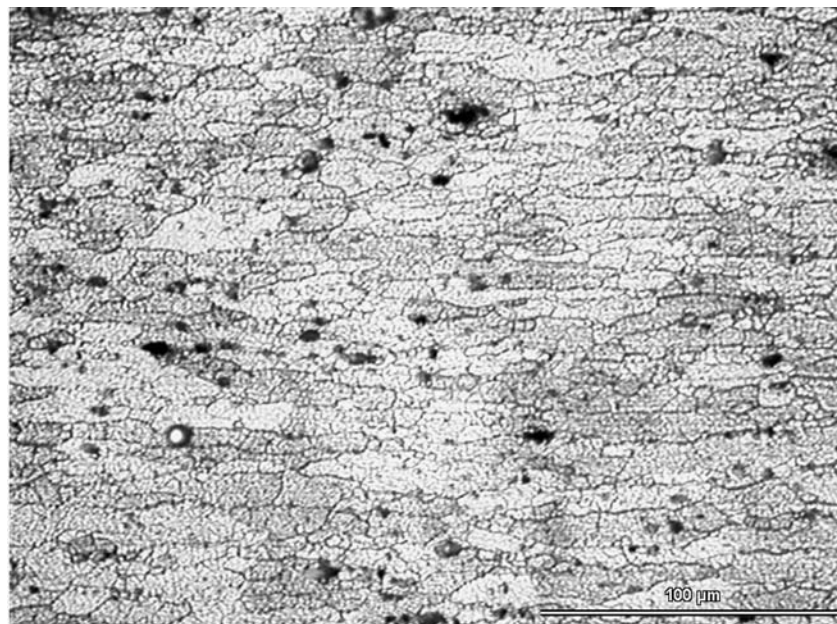
(b)

Figure 3 Fine recrystallized grains observed at a distance of 2 mm from the weld centre of the studied joints.

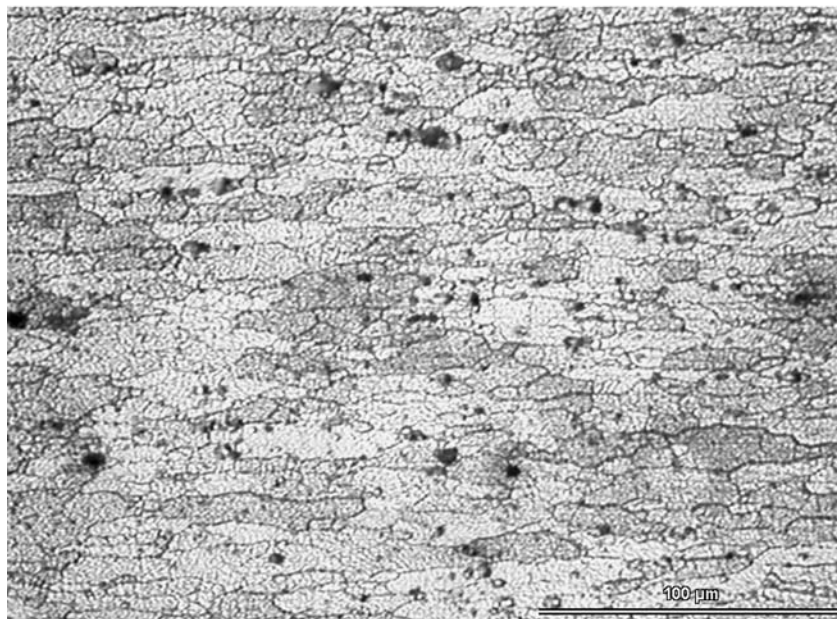
condition. Both material sheets measured 2.5 mm thick. The longitudinal direction of the FSW was perpendicular to the rolling direction of 2024 aluminium alloy and parallel to the rolling direction of 7075 one, this lay out of the joints was chosen to simulate a more drastic mechanical condition respect to the classical welds found in literature in which both sheets are welded with the same rolling direction even in the case of different parent materials. The rotating speed of the tool was 700 RPM while the welding speed was 2.67 mm/s, the steel tool was rotated in the clockwise direction while the specimens, fixed at the backing plate, were moved. The nib was 6 mm in diameter and 2.5 mm long, and a 20 mm diameter shoulder was machined perpendicular to the axis of the tool; the tilt angle of the tool was 3°. The 7075 alloy was on the advancing side of the tool while the 2024 alloy was on the retreating one.

The Vickers hardness profile of the weld zone was measured on a cross-section and perpendicular to the welding direction using a Vickers indenter with a 200 gf load for 15 s.

Tensile tests were performed in order to evaluate the mechanical properties of the joints obtained by FSW process of the two different materials of the present study. Tensile test specimens were sectioned in the longitudinal and transverse direction respect to the weld line with an electrical discharge machine (EDM). The gage dimensions of the specimens, in transverse direction, were 40 mm in length and 16 mm in width respectively while the gage dimensions of the specimens in longitudinal direction were 10 mm in length and 4 mm in width. All the specimens were mechanically polished before tests in order to eliminate the effect of possible surface irregularities. The tensile test was carried out at



(a)



(b)

Figure 4 Grains of the parent material appearing at a distance of 4 mm from the weld centre of the joints.

room temperature using an MTS 810 testing machine with initial strain rate of 10^{-3} s^{-1} .

Endurance fatigue tests were performed on a resonant electro-mechanical testing machine under constant loading control up to 250 Hz sine wave loading TESTRONICTM $50 \pm 25 \text{ KN}$, produced by RUMUL (SUI). The cyclic fatigue tests were conducted in the axial total stress-amplitude control mode under fully-reversed, push-pull, tension loading ($R = \sigma_{\min}/\sigma_{\max} = 0.1$). All mechanical tests were performed up to failure. Surfaces were prepared by standard metallographic techniques and etched with Keller's reagent and grain structure of the weld zone was characterized by optical microscopy. A scanning electron microscope equipped with field emission gun (JEOL-JSM 6500 F) was employed for the observation of the fracture surfaces of the specimens tested in monothonic and cyclic loading

in order to study the microscopic defects of the joints and the mechanisms involved during deformation.

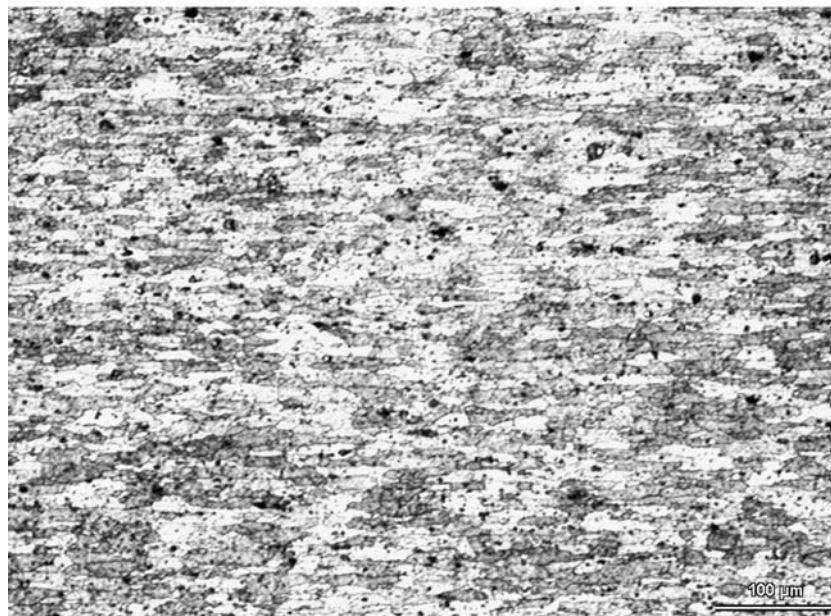
3. Results and discussion

In the present study dissimilar materials, 2024 and 7075 aluminium alloy were successfully joined by FSW and no superficial porosity or defects were observed in both weld top and rear surface.

Light microscopy observations were widely performed on the transverse cross-sections of the specimens, the FSW process of the 2024 and 7075 aluminium alloys revealed the classical formation of the elliptical "onion" structure in the centre of the weld; this is a structure characterized by fine recrystallized grains. The thermo-mechanical effected zone (TMAZ) is evident from optical microscopy observations (Fig. 1). The



(a)



(b)

Figure 5 TMAZ zone grains (a) and parent material grains (b): the grains dimensions difference is clearly distinguished in the studied joints.

micro hardness profile along the FSW joint is shown in Fig. 2, the micro hardness reaches a value of 150 Hv in the centre of the weld and after increasing in both the 2024 and 7075 sides it starts to decrease after 2 mm from the centre until reaching a plateau corresponding to the hardness values of the parent materials. The hardness of the joint reaches lower values in the HAZ respect to the parent material in both 2024 and 7075 sides, this is a classical behaviour in the aluminium alloys welded by FSW, in the HAZ and TMAZ, in fact, the competing mechanisms of work hardening and over-ageing produce a strength decreasing respect to the stirred zone and the base metal. The micrograph, shown in Fig. 3 represents a section perpendicular to the welding direction, the “nugget” zone that consists of very fine grains. The higher temperature and severe plastic deformation results in grains smaller than the base metal. In all the FSW literature on aluminium

loys, the initial elongated grains of the parent materials are converted to a new equiaxed fine grain structure. At higher magnifications the optical micrographs showed very fine equiaxed grains in the recrystallized zones (Fig. 3). These photomicrographs were taken at 2 mm in the zone of the higher micro hardness value measured from the AA7075 side. By moving away from the weld centre, the grains dimensions increase and the grains begin to result less equiaxed than those closer to the weld centre (Fig. 4). At a distance of 4 mm from the weld centre many of the prior grains of the parent material start to appear. This region corresponds to the heat affected zone as the hardness is low compared to the base metal. The hardness drops here because the precipitates are coarsened as discussed by Jata *et al.* [3]. In the region adjacent to the nugget, i.e. TMAZ no recrystallization is observed because the temperature derived from the friction stir processing is not high



(a)



(b)

Figure 6 Optical micrograph at a distance from the weld centre of 2 mm (a) and 3 mm (b) in the 2024 side of the joints.

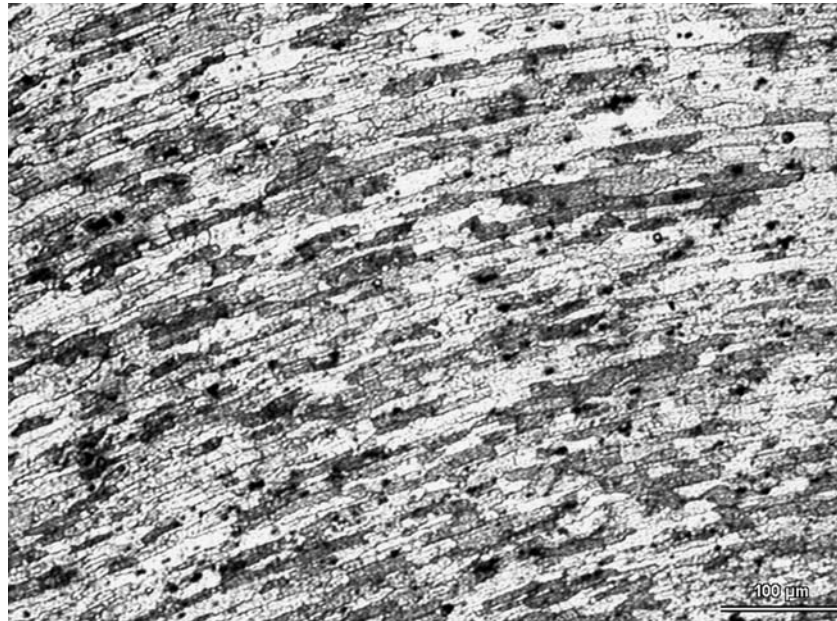


Figure 7 Grains from the TMZ zone in the 2024 side.

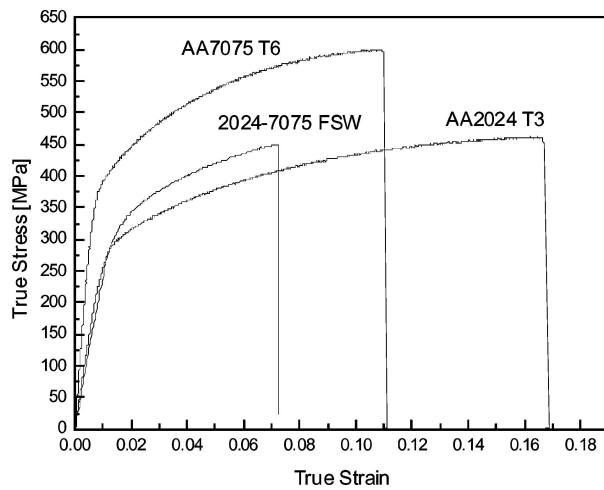


Figure 8 True Stress vs. True Strain curve of the studied joints tested in tension.

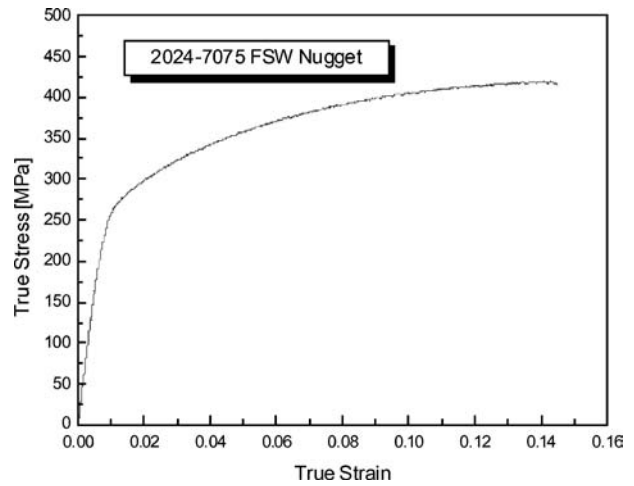


Figure 9 True Stress vs. True Strain tensile behaviour of the FSW joints parallel to the welding direction.

enough and the deformation is not so severe to cause recrystallization. Fig. 5a, shows the deformed grains in the TMAZ and the regions adjacent to the TMAZ is the HAZ, Fig. 5b, where the grain size is similar to the base metal. However the hardness in the HAZ is low. Similar microstructural observations were made in the FSW zone of the 2024 side of the weld. Photographs shown in Fig. 6 and correspond to the grains in the nugget at a distance of 2 mm from the weld center line and 6b corresponds to the grains 3 mm away from the center line. Fig. 7 shows the grains in the TMAZ where the grains are severely bent from deformation but recrystallization was absent.

The tensile response, transverse to the welding direction, of the 2024 and 7075 AA joined by FSW is shown in Fig. 8. The curve exhibits a classical behaviour and the mechanical properties, compared to the parent metals, are reported in Table I. The joint exhibits very good properties of yielding, UTS and ductility from a global point of view even if the weld has lower 0.2% proof stress and elongations respect to the base metals, the

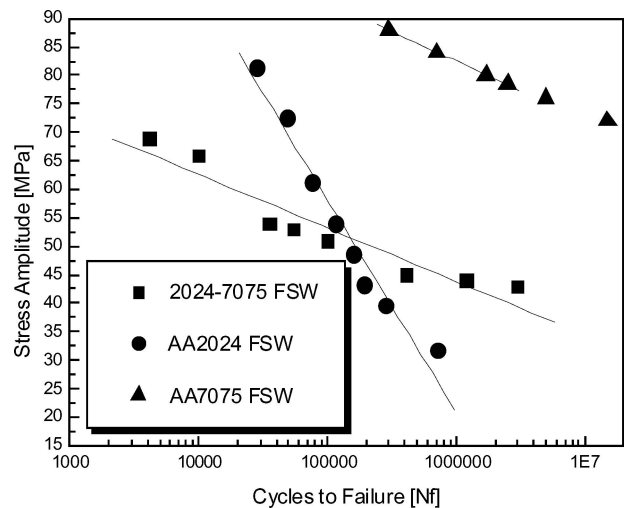


Figure 10 Endurance Fatigue curves (S-N) of the 2024-7075 plates joined by Friction Stir Welding compared with the Friction Stir Welded AA2024 T3 and AA7075 T6.

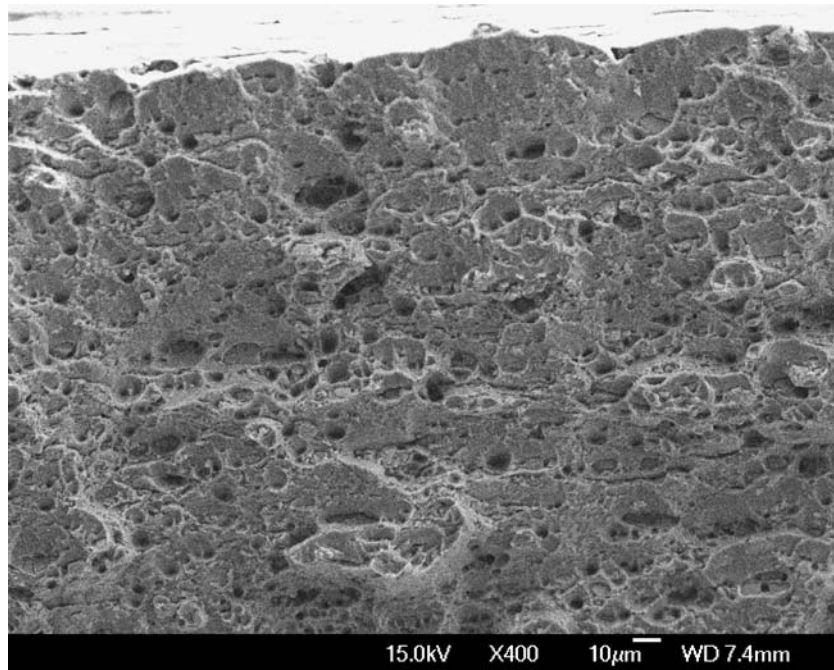


Figure 11 Tensile specimen fracture surface of the studied joint showing voids population.

mechanical results are very good considering the drastic conditions to which the materials are subjected during the Friction Stir Welding process, the elastic modulus results very different respect to the parent materials. The specimens fractured in the HAZ zones of the welds, always close to the 2024 material. This demonstrates the classical behaviour of these kind of joints in which, from a microstructural point of view, the mechanical response of the centre of the weld results higher and higher respect to the parent material and the HAZ because of the large grains dimensions differences. In this zone, in fact, the mean grain equivalent diameter measured by optical images resulted $2.5 \mu\text{m}$.

The room temperature tensile behaviour of the material of the nugget zone is shown in Fig. 9. The strength and ductility of the material results strongly increased in the nugget zone respect to the material in the transverse direction thanks to the uniform and very fine structure consequent to the friction Stir process.

The curve representing the stress amplitude-fatigue life response of the welded material and of the 2024 parent alloy is reported in Fig. 10, the curve shows a classical behaviour for the aluminium alloys, revealing a trend of increasing fatigue life with decreasing cyclic stress amplitude.

A fatigue life of 3×10^6 cycles at 73 MPa was recorded for the weld joints of the present study. The fatigue curve shows very good results compared with the stress levels reached by the parent unwelded material at the same test frequency, considering the critical sit-

uation exhibited by welded joints in aluminium alloys subjected to cyclic loading [20], in particular, if compared with the 2024 T3 and the 7075 T6 alloys after Friction Stir Welding, the 2024–7075 joints show a decrease in fatigue life respect the FSW 7075 T6 ones while show a net increase in fatigue life respect to the 2024 T3 FSW joints in the High Cycle Regime.

In the understanding of microstructural effects on fracture properties, the observation of fractured surfaces results fundamental.

The fracture surface of the 2024–7075 joints tested in tension was covered with a broad population of microscopic voids of different size and shape (Fig. 11), at room temperature the material showed ductility with fracture, the observations performed by employing FEGSEM revealed locally ductile mechanisms.

4. Conclusions

The 2024 and 7075 aluminium alloys were successfully joined together by friction stir welding 2.5 mm thick sheets. The resulting microstructure was widely investigated by optical microscopy putting in evidence the grain structure differences resulting by the process. The mechanical properties of the joints were evaluated by tensile showing a net increase in strength in longitudinal direction respect to the transverse one; fatigue tests showed an increase in fatigue life in the High Cycle Regime respect to the FSW 2024 T3 joints and a decrease in fatigue life respect to the FSW 7075 T6 ones.

References

1. G. BUSSU and P. E. IRVING, *Intern. J. Fatigue* **25** (2003) 77.
2. R. JOHN, K. V. JATA and K. SADANANDA, *ibid.* **25** (2003) 939.
3. K. V. JATA, K. K. SANKARAN and J. RUSCHAU, *Metall. Mater. Trans.* **31A** (2000) 2181.

TABLE I Mechanical properties of the 2024-7075 joints compared with those proper of the parent materials

Material	σ_y (MPa)	UTS (MPa)	Elomgation (%)
AA2024	380	490	17
AA7075	503	572	11
2024-7075 FSW	325	424	6

4. I. CHARIT, R. S. MISHRA and M. W. MAHONEY, *Scripta Materialia* **47** (2002) 631.
5. H. G. SALEM, A. P. REYNOLDS and J. S. LYONS, *ibid.* **46** (2002) 337.
6. C. G. RHODES, M. W. MAHONEY, W. H. BINGEL and M. CALABRESE, *ibid.* **48** (2003) 1451.
7. K. V. JATA and S. L. SEMIATIN, *ibid.* **43(8)** (2000) 743.
8. W. D. LOCKWOOD, B. TOMAZ and A. P. REYNOLDS, *Mater. Sci. Engng.* **A323** (2002) 348.
9. M. GUERRA, C. SCHMIDT, J. C. MCCLURE, L. E. MURR and A. C. NUNES, *Mater Character.* **49** (2003) 95.
10. P. ULYSSE, *Intern. J. Machine. Tools Manuf.* **42** (2002) 1549.
11. J.-Q. SU, T. W. NELSON, R. MISHRA and M. MAHONEY, *Acta. Materialia* **51** (2003) 713.
12. C. G. RHODES, M. W. MAHONEY and W. H. BINGEL, *Scripta Mater.* **36** (1997) 69.
13. (a) I. SHIGEMATSU, Y. J. KWON, K. SUZUKI, T. IMAI and N. SAITO, *J. Mater. Sci. Lett.* **22** (2003) 353; (b) YING LI, L. E. MURR and J. C. MCCLURE, *Mater. Sci. Engng.* **A271** (1999) 213.
14. (a) YUTAKA S. SATO, MITSUNORI URATA, HIROYUKI KOKAWA and KEISUKE IKEDA, *ibid.* **A354** (2003) 298; (b) PATRICK B. BERBON, WILLIAM H. BINGEL, RAJIV S. MISHRA, CLIFFORD C. BAMPPTON and MURRAY W. MAHONEY, *Scripta Mater.* **44** (2001) 61.
15. WON-BAE LEE, YUN-MO YEON and SEUNG-BOO JUNG, *ibid.* **49** (2003) 423.
16. HUSEYIN UZUN, CLAUDIO DALLE DONNE, ALBERTO ARGAGNOTTO, TOMMASO GHIDINI and CARLA GAMBERO, *Mater. Des.* **26** (2005) 41.
17. YUTAKA S. SATO, SEUNG HWAN C. PARK, MASATO MICHUUCHI and HIROYUKI KOKAWA, *Scripta Mater.* **50** (2004) 1233.
18. W. B. LEE, Y. M. YEON and S. B. JUNG, *Mater. Sci. Engng.* **A355** (2003) 154.
19. YING LI, E. A. TRILLO and L. E. MURR, *J. Mater. Sci. Lett.* **19** (2000) 1047.
20. S. LOMOLINO, R. TOVO and J. DOS SANTOS, *Inter. J. Fatig.* **27** (2005) 305.

*Received 12 October 2004
and accepted 11 February 2005*